Theory and Gyro-fluid Simulations of Edge-Localized-Modes[1]

X. Q. Xu[1], P. W. Xi[1,2], A. Dimits[1], I. Joseph[1], M. V. Umansky[1], T. Y. Xia[1,3], B. Gui[1,3], S. S. Kim[4], G. Y. Park[4], T. Rhee[4], H. Jhang[4], P. H. Diamond[4,5], B. Dudson[6], P. B. Snyder[7]

[1)] Lawrence Livermore National Laboratory, Livermore, CA 94550 USA
[2)] School of Physics, Peking University, Beijing, China
[3)] Institute of Plasma Physics, Chinese Academy of Sciences, Hefei, China
[4)] WCI Center for Fusion Theory, National Fusion Research Institute, Daejon, R. Korea
[5)] Center for Astrophysics and Space Sciences and Department of Physics, University of California San Diego, La Jolla, CA 92093-0429, USA
[6)] University of York, Heslington, York YO10 5DD, UK
[7)] General Atomics, San Diego, CA 92186 USA

e-mail contact of main author: `xxu@llnl.gov`

Abstract. This paper reports on the theoretical and simulation results of a gyro-Landau-fluid (GLF) extension of the BOUT++ code which contributes to increasing the physics understanding of edge-localized-modes (ELMs). Large ELMs with low-to-intermediate-n peeling-ballooning (P-B) modes are significantly suppressed due to finite Larmor radius (FLR) effects when the ion temperature increases. For type-I ELMs, it is found from linear simulations that retaining complete first order FLR corrections as resulting from the incomplete "gyroviscous cancellation" in Braginskii's two-fluid model is necessary to obtain good agreement with gyro-fluid results for high ion temperature cases ($T_i \succeq 3keV$) when the ion density has a strong radial variation, which goes beyond the simple local model of ion diamagnetic stabilization of ideal ballooning modes. The maximum growth rate is inversely proportional to T_i because the FLR effect is proportional to T_i. The FLR effect is also proportional to toroidal mode number n, so for high n cases, the P-B mode is stabilized by FLR effects. Nonlinear gyro-fluid simulations show results that are similar to those from the two-fluid model, namely that the P-B modes trigger magnetic reconnection, which drives the collapse of the pedestal pressure. Hyper-resistivity is found to limit the radial spreading of ELMs by facilitating magnetic reconnection. Due to the additional FLR-corrected nonlinear ExB convection of the ion gyro-center density, the gyro-fluid model further limits the radial spreading of ELMs. Because edge plasmas have significant spatial inhomogeneities and complicated boundary conditions, we have developed a fast non-Fourier method for the computation of Landau-fluid closure terms based on an accurate and tunable approximation. The accuracy and the fast computational scaling of the method have been demonstrated.

1. Introduction

This paper reports on the theoretical and simulation results of a Gyro-Landau fluid (GLF) extension of the BOUT++ code which contributes to increasing the physics understanding of edge-localized-modes (ELMs). The large ELMs with low-to-intermediate-n peeling-ballooning (P-B) modes are significantly suppressed due to finite Larmor radius (FLR) effects when the ion temperature increases.

An isothermal truncation of the electromagnetic gyro-fluid model of Snyder and Hammett [1] is developed for ELM simulations. The ion gyrocenter density and electron density are

[1]This work was performed for USDOE by LLNL under Contract DE-AC52-07NA27344, grants DE-FG03-95ER54309 at general Atomics, and by the UK Engineering and Physical Sciences Research Council under grant EP/H012605/1 and the Euro. Commun. under the contract of Association between EURATOM and CCFE.

combined to yield a gyro-kinetic vorticity density equation. The set of nonlinear electromagnetic gyro-fluid equations consists of gyro-kinetic vorticity density, ion gyrocenter density, the generalized Ohms law and Ampere's law. The simple set of gyro-fluid equations correctly describes a range of plasma instabilities relevant to edge plasmas, such as low-to-intermediate-n peeling-ballooning modes and high-n drift-ballooning modes. The first-order Padé's approximation to $\Gamma_0(b) = 1/(1+b)$ is used to get the potential by inverting the gyrokinetic vorticity density. In the limit of small ion gyro-radius length, $b = k_\perp^2 \rho_i^2 \ll 1$ (to first order finite Larmor radius approximation in b), this set of equations is shown to be the same as the two-fluid model that includes finite Larmor radius (FLR) effects. We demonstrate that the complicated nonlinear gyro-viscous tensor in the two-fluid model naturally appears in the isothermal gyro-fluid model as the FLR-corrected ExB convection for the ion gyro-center density in the gyro-kinetic vorticity density equation and the FLR-corrected gyro-kinetic vorticity density. This offers a simple, yet adequate description of ion dynamics that is relatively easy to implement in nonlinear simulation codes. We also show that the gyro-kinetic vorticity density is the charge density only in the cold-ion limit.

Because edge plasmas have significant spatial inhomogeneities and complicated boundary conditions, it is desirable to compute the closure terms in configuration space. The nonlocality of Landau-fluid operators can make the naive direct computations of the closure terms in configuration space via convolution or matrix multiplication very expensive. We have therefore developed a fast non-Fourier method for the computation of Landau-fluid closure terms based on an accurate and tunable approximation that can be numerically implemented through the solution of matrix equations in which the matrices are tridiagonal or narrowly banded. The accuracy, for the operator itself and for the resulting plasma response function and the fast computational scaling of the method have been demonstrated. A spectral collocation analysis has been developed that greatly aids in the optimization of the approximations for accuracy and computational cost, both for cases that are collisionless and for cases where collisional and collisionless damping processes compete.

The organization of this paper is as follows. The basic set of equations and isothermal simulation model are given in Sect. 2. Nonlinear simulation of Peeling-Ballooning modes is discussed in Sect. 3. A new non-Fourier Method for applying the Landau-Fluid operators are given in Sect. 4. Summary and discussion are given in Sect. 5.

2. An isothermal electromagnetic 3-field gyro-fluid model

To begin, a simple reduced set of gyro-fluid equations can be obtained by assuming that the equilibrium ion and electron temperatures are constant and equal, and ions and electrons are isothermal. The isothermal 3-field gyro-fluid model can be obtained from Snyder-Hammett model [1] with the generalized Poisson equation and the generalized Ohm's law:

$$\frac{\partial n_{iG}}{\partial t} + \mathbf{v}_{EG} \cdot \nabla n_{iG} = -\left(\frac{2}{eB}\right) \mathbf{b_0} \times \kappa \cdot \nabla p_{iG} \tag{1}$$

$$\frac{\partial n_e}{\partial t} + \mathbf{v}_E \cdot \nabla n_e = \left(\frac{2}{eB}\right) \mathbf{b_0} \times \kappa \cdot \nabla p_e - \nabla_\parallel \left(n_e v_{\parallel e}\right), \tag{2}$$

$$\frac{\partial A_\parallel}{\partial t} = -\partial_\parallel \phi + \frac{1}{n_e e} \partial_\parallel p_e + \frac{\eta}{\mu_0} \nabla_\perp^2 A_\parallel - \frac{\eta_H}{\mu_0} \nabla_\perp^4 A_\parallel \tag{3}$$

$$J_{||} = -\frac{1}{\mu_0} \nabla_\perp^2 A_\parallel = -n_e e v_{\parallel e}, \tag{4}$$

$$n_e = \bar{n}_i - n_i\left[1-\Gamma_0(b)\right]\frac{Z_i e\phi}{T_0} + n_i\rho_i^2\left(\nabla_\perp \ln n_i\right)\cdot\nabla_\perp\left[\left(\Gamma_0-\Gamma_1\right)\left(\frac{Z_i e\phi}{T_0}\right)\right], \quad (5)$$

$$\bar{n}_i = \Gamma_0(b)^{1/2} n_{iG}, \qquad b = -\rho_i^2\nabla_\perp^2. \quad (6)$$

where $\bar{n}_i$ is the gyro-phase independent part of the real space ion density. The notation n_{iG} is the ion gyro-center density and n_i is the particle density (equal to n_e in the limit of small Debye length, $k\lambda_D \ll 1$). For the various definitions of density, the relation between the particle and gyro-center representations is given by the gyro-kinetic Poisson equation, Eq. (5). Definitions of various quantities associated with plasma physics are as follows:

$$\mathbf{v}_{EG} = \mathbf{b}_0\times\nabla_\perp\Phi_G/B, \qquad \mathbf{v}_E = \mathbf{b}_0\times\nabla_\perp\phi/B, \qquad \tilde{\mathbf{B}} = \nabla A_\parallel\times\mathbf{b}_0. \quad (7)$$

The notation $\Phi_G = \bar{\Phi} = \Gamma^{1/2}(b)\phi$ has been introduced for gyro-averaged electric potential. Here $\nabla_\parallel F = B\partial_\parallel(F/B)$ for any F, $\partial_\parallel = \partial_\parallel^0 + \tilde{\mathbf{b}}\cdot\nabla, \tilde{\mathbf{b}} = \tilde{\mathbf{B}}/B, \partial_\parallel^0 = \mathbf{b_0}\cdot\nabla, \kappa = \mathbf{b_0}\cdot\nabla\mathbf{b_0}$, η is resistivity and η_H hyper-resistivity, also known as electron viscosity. The symbol tilde represents the fluctuation quantities.

Since in the long wavelength regime of a quasi-neutral plasma $\bar{n}_i$ and n_e are two large numbers and are almost equal $\bar{n}_i \sim n_e$ and Eq. (5) can be rewritten as $1-\bar{n}_i/n_e \simeq (k_\perp\rho_i)^2 e\phi/T_e$, where $(k_\perp\rho_i)^2 \ll 1$ and $e\phi/T_e \sim 1$, the desired solution of Poisson equation as written depends on the difference of two large and almost equal numbers. Therefore it is difficult to accurately obtain numerical solutions when n_{iG} and n_e evolve separately because the numerical errors in $(\bar{n}_i(\mathbf{x},t) - n_e(\mathbf{x},t))$ may be on the same order as the ion polarization density.

Here we propose an alternative formulation. We define two new variables: gyrokinetic vorticity density $\varpi_G = eB(n_e - n_{iG})$ and gyrokinetic total pressure $p_G = p_{iG} + p_e = n_{iG}T_{iG} + n_eT_e = (n_{iG}+n_e)T_0$, assuming electron temperature T_e being equal to ion temperature T_{iG} $T_e = T_{iG} = T_0$. For the isothermal model, which neglects all considerations of temperature dynamics, we can rewrite the gyrokinetic vorticity density as

$$\frac{\partial\varpi_G}{\partial t} + \mathbf{v}_E\cdot\nabla\varpi_G - eB(\mathbf{v}_{EG}-\mathbf{v}_E)\cdot\nabla n_{iG} = 2\mathbf{b_0}\times\kappa\cdot\nabla p_G + B\nabla_\parallel j_\parallel, \quad (8)$$

$$\frac{\partial p_G}{\partial t} + \mathbf{v}_E\cdot\nabla p_G + T_0(\mathbf{v}_{EG}-\mathbf{v}_E)\cdot\nabla n_{iG} = 0, \quad (9)$$

$$\varpi_G = eB\left\{\Gamma_0^{1/2}(b)n_{iG} - n_{iG} - n_i\left[1-\Gamma_0(b)\right]\left(\frac{Z_i e\phi}{T_0}\right)\right\} + n_i eB\rho_i^2\nabla_\perp\ln n_i\cdot\nabla_\perp\left[\left(\Gamma_0-\Gamma_1\right)\left(\frac{Z_i e\phi}{T_0}\right)\right], \quad (10)$$

$$n_e = \frac{1}{2}\left(\frac{p_G}{T_0} + \frac{\varpi_G}{eB}\right), \qquad n_{iG} = \frac{1}{2}\left(\frac{p_G}{T_0} - \frac{\varpi_G}{eB}\right), \qquad p_e = n_eT_0. \quad (11)$$

Here the parallel current term and the diamagnetic flow when $T_i \neq T_e$ have been neglected in pressure equation. The conlisional stress tensors can easily be included in connection to fluid descriptions. The equations for $A_\parallel$ and $J_\parallel$ are the same as in Eqs. (3) and (4). This formulation naturally couples different domains (core, the SOL and the private flux region) together in the edge region through boundary conditions. Otherwise, it is not obvious how to impose the parallel sheath boundary conditions for electrostatic potential ϕ at the divertor plates if the generalized Poisson equation (5) is solved directly because full parallel physics does not enter into this equation.

2.1 Gyro-fluid vorticity density equation in the limit of small ion gyro-radius length

In the long-wavelength limit where $(k_\perp \rho_i)^2 \ll 1$, $\Gamma_0(b) = 1/(1+b) \simeq 1-b, \Gamma_0^{1/2}(b) = 1/(1+b/2) \simeq 1-b/2, \Gamma_0 - \Gamma_1 \simeq (1-b/2)/(1+b) \simeq 1-3b/2, \Phi_G - \phi = (1/2)\rho_i^2 \nabla_\perp^2 \phi$. The 3-field gyro-fluid model in the limit of small ion gyro-radius length becomes

$$\frac{\partial \varpi_G}{\partial t} + \mathbf{v}_E \cdot \nabla \varpi_G - \frac{eB}{2T_0}\rho_i^2 \left[\frac{\mathbf{b}_0 \times \nabla_\perp (\nabla_\perp^2 \phi)}{B}\right] \cdot \nabla p_{iG} = 2\mathbf{b_0} \times \kappa \cdot \nabla p_G + B\nabla_\parallel j_\parallel. \quad (12)$$

$$\frac{\partial p_G}{\partial t} + \mathbf{v}_E \cdot \nabla p_G + \frac{1}{2}\rho_i^2 \left[\frac{\mathbf{b}_0 \times \nabla_\perp (\nabla_\perp^2 \phi)}{B}\right] \cdot \nabla p_{iG} = 0, \quad (13)$$

$$\varpi_G = \frac{eB}{T_0}\rho_i^2 \left[n_i Z_i e \nabla_\perp^2 \phi + n_i Z_i e \nabla_\perp \ln n_i \cdot \nabla_\perp \phi + \frac{1}{2}\nabla_\perp^2 p_{iG}\right]. \quad (14)$$

The equations for $A_\parallel$, $J_\parallel$, n_e, n_{iG}, and p_e are the same as Eq. (3), (4), and (11), respectively. By defining the two-fluid vorticity density $\varpi = \omega_{ci}[\varpi_G + (eB/2T_0)\rho_i^2 \nabla_\perp^2 p_{iG}]$, this equation can be rewritten into the form which is the same as two-fluid version of vorticity equation (2) given by Xu et al [2], excluding external momentum sources and collisional ion viscosity, which is given here again for comparison and will be later referred as two-fluid model in simulation sections:

$$\begin{aligned}\frac{\partial \varpi}{\partial t} &+ \left(\mathbf{v}_E + v_{\parallel i}\mathbf{b}_0\right) \cdot \nabla \varpi = (2\omega_{ci})\, \mathbf{b_0} \times \kappa \cdot \nabla p + n_i Z_i e \frac{4\pi v_A^2}{c^2} \nabla_\parallel j_\parallel \\ &- \frac{1}{2}\left\{n_i Z_i e \mathbf{v}_{pi} \cdot \nabla(\nabla_\perp^2 \phi) + \mathbf{v}_E \cdot \nabla(\nabla_\perp^2 p_i) - \nabla_\perp^2 [\mathbf{v}_E \cdot \nabla(p_i)]\right\}\end{aligned} \quad (15)$$

It should be noted, however, that Eq. (15) is written in CGS unites as the original paper [2], while SI units are used in this paper. This resolves the long-standing issue regarding the difference in vorticity equation derived from two-fluid and gyrokinetic framework. The gyro-viscous terms emerge naturally from the FLR nonlinearities in the ion gyrocenter density in the limit of small ion gyro-radius length. Furthermore, the gyro-fluid equations show a simple physics picture and can be easily implemented in simulation codes. The one-half of ion diamagnetic drift vorticity in ϖ_G [the last term on the right-hand-side of Eq. (14)] indicates that the gyro-kinetic vorticity density ϖ_G is the charge density only in the cold-ion limit.

2.2 Gyro-fluid equilibrium and axisymmetric component of fluctuations

Ion equilibrium with subsonic flow velocity $\mathbf{v}_i$, can be characterized by the force balance relation $n_i Z_i e \nabla \Phi + \nabla P_i = Z_i e n_i \mathbf{v}_i \times \mathbf{B}$. The parallel two-fluid vorticity (or simply two-fluid vorticity) $\varpi = \omega_{ci}\mathbf{b} \cdot \nabla \times (n_i m_i \mathbf{v}_i)$ therefore can be written as $\varpi = n_i Z_i e \nabla_\perp^2 \Phi + n_i Z_i e \nabla_\perp \ln n_i \cdot \nabla_\perp \Phi + \nabla_\perp^2 P_i$. For a typical ion equilibrium with subsonic ion flow velocity and with weak ion temperature gradient in H-mode pedestal plasmas, the ExB drift is balanced with ion diamagnetic drift, the equilibrium vorticity is almost zero, $\varpi_0 \simeq 0$, which yields the isothermal relation $Z_i e \Phi_0 \simeq T_0 \ln P_{i0}$.

Therefore to lowest order of the poloidal ion gyroradius to the ion temperature scale ($\rho_{pi}/L_{Ti} \ll 1$), subsonic ion flow implies that the pedestal is maintained by a large electron current with the ions electrostatically confined. Since the two-fluid vorticity is different from gyro-fluid vorticity by one-half of ion diamagnetic drift vorticity, for typical subsonic ion flow force

balance means a non-zero gyro-fluid equilibrium vorticity,

$$\varpi_{G0} = -\left(\frac{eB}{2T_0}\right)\rho_i^2\nabla_\perp^2 P_{i0}. \tag{16}$$

Similarly for the isothermal model, if we assume that the turbulence-generated steady-state axisymmetric component of ion flow is subsonic ($\langle v_{i\perp}\rangle_\zeta \ll v_{Ti}$), the same isothermal relation holds for gyro-fluid model as well $Z_i e\Phi \simeq T_0 \ln(P_{i0} + \langle p_i\rangle_\zeta)$. Here $\langle p_i\rangle_\zeta$ means the axisymmetric component of ion pressure fluctuations, i.e. n=0 component. The same is true for the turbulence-generated axisymmetric component of gyro-fluid vorticity:

$$\langle\varpi\rangle_\zeta = 0 \qquad \Longrightarrow \qquad \langle\varpi_G\rangle_\zeta = -\left(\frac{eB}{2T_0}\right)\rho_i^2\nabla_\perp^2\langle p_{iG}\rangle_\zeta. \tag{17}$$

In other words, we assume that the ion response is adiabatic for both equilibrium and steady-state axisymmetric component of fluctuations.

3. ELM Gyro-fluid Simulations

Utilizing a Padé approximation for the modified Bessel functions, this set of equations (1)-(6) is implemented in the BOUT++ framework with full ion FLR effects, except that $\Gamma_0 - \Gamma_1 \simeq 1$ is used in the last term of Eq.(5) for ELM simulations, where we assume $k_\perp L_n \gg 1$. This simple isothermal 3-field gyro-fluid model does not yet include Landau damping for peeling-ballooning (P-B) modes with $\omega \sim \omega_{*i} \gg \omega_{ti}$ where ω_{*i} is the ion diamagnetic drift frequency and $\omega_{ti} = v_{ti}/qR$ is the thermal ion transit frequency.

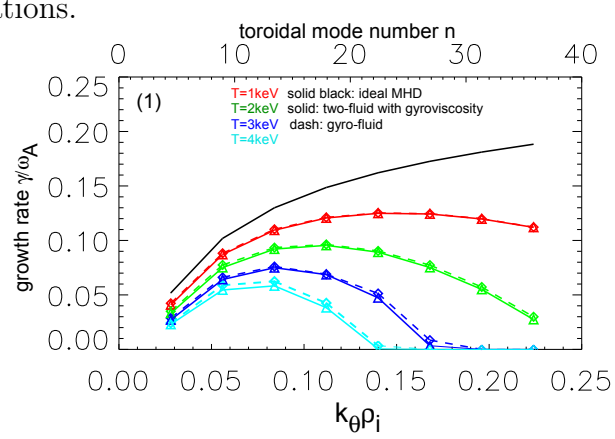

FIG. 1: The influence of the FLR physics on the linear growth rate of P-B modes versus toroidal mode number n (top) or poloidal wavelength normalized to ion Larmor radius $k_\theta\rho_i$ (bottom, calculated with $T_0 = 1keV$ for the ideal MHD P–B mode (black), with two-fluid retaining the complete first-order FLR corrections (solid), and with gyro-fluid full FLR effects (dash) for different plasma temperature T_i.

To study the physics of nonlinear P-B mode dynamics, we choose circular cross-section toroidal equilibria with an aspect ratio of 2.9 generated by the TOQ equilibrium code. The plasma equilibrium is far from the marginal P-B instability threshold with a pedestal toroidal pressure $\beta_{t0} = 1.941 \times 10^{-2}$ and a normalized pedestal width $L_{ped}/a = 0.0486$ [3,4]. In this study, the resistivity η, hyper-resistivity η_H and edge temperature T_0 are treated as constants in space-time across simulation domain. Except in Sect. 3.3 to investigate the influence of equilibrium shear flow on peeling-ballooning instability and edge localized mode crash, in the present simplified models in Sect. 3.1 and 3.2, both equilibrium flow and turbulent zonal flow have been set to be zero for both two-fluid and gyro-fluid models in BOUT++ code: $\mathbf{V}_0 = \mathbf{V}_{E0} + \mathbf{V}_{\nabla P_i} = 0$ and $\langle\delta\mathbf{v}\rangle_\zeta = \langle\mathbf{v}_E\rangle_\zeta + \langle\mathbf{v}_{\nabla P_i}\rangle_\zeta = 0$. Therefore, the equilibrium electric field is $E_{r0} = (1/n_0 Z_i e)\nabla_r P_{i0}$ with ion pressure $P_{i0} = P_0/2$, and the perturbed electric field is $\langle E_r\rangle_\zeta = (1/n_0 Z_i e)\nabla_r\langle P_i\rangle_\zeta$. The zonal magnetic field is also set to be zero as it is negligibly small compared to the equilibrium magnetic field B_0. Radial boundary conditions used are: $\varpi = 0, \nabla_\perp^2 A_\parallel = 0, \partial P/\partial\psi = 0$, and $\partial\phi/\partial\psi = 0$ on inner radial boundary; $\varpi = 0, \nabla_\perp^2 A_\parallel = 0, P = 0$, and $\phi = 0$ on outer radial boundary. The domain is periodic in parallel coordinate y (with a twist-shift condition) and periodic in binormal coordinate z.

For efficiency, when performing nonlinear simulations, only 1/5th of the torus is simulated. The number of grid cells in each coordinate are $n_\psi = 512, n_y = 64$, and $n_z = 32$.

3.1 Linear Gyro-fluid Simulations

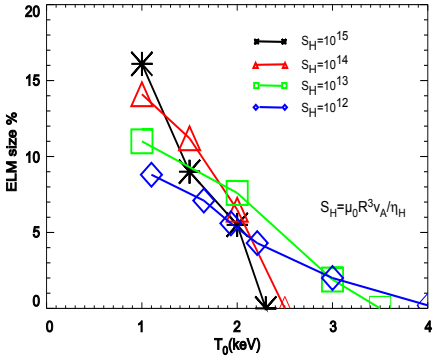

FIG. 2: ELM size vs ion temperature T_i and hyper-resistivity η_H for constant density case. Lundquist number $S = \mu_0 R_0 v_A/\eta = 10^8$.

The initial simulation results are shown to be consistent with the previous two-fluid model including only the ion diamagnetic drift for constant density profile. Retaining the complete first-order FLR corrections (including all three terms on the second line of Eq.(15)) is necessary to obtain good agreement with gyro-fluid results for high ion temperature cases ($T_i \succeq 3keV$) when the ion density has a strong radial variation. The influence of gyro-radius effects on the linear growth rate of P-B modes vs. n (top) and $k_\theta \rho_i$ (bottom, calculated with T_i=1kev) is summarized in Fig.1 for type-I ELMs. Good agreement in the linear growth rate is shown in long-wavelength limit between the ideal MHD model (black), two-fluid model (solid), and gyro-fluid model (dash). In both cases, the maximum growth rate is inversely proportional to T_i because the FLR effect is proportional to T_i. The FLR effect plays the role of a threshold in the growth rate. Only the perturbations with a growth rate higher than the threshold become unstable. Therefore, as the ion temperature increases, the FLR and the stabilizing effect increase. The FLR effect is also proportional to toroidal mode number n, so for high n cases, the peeling-ballooning mode is stabilized by FLR effects.

3.2 Nonlinear Gyro-fluid Simulations

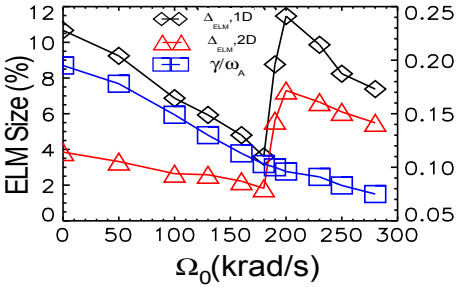

FIG. 3: ELM size versus flow amplitude Ω_0. The flow shear scale length $L_v = 3.4cm$. The blue line is the mode growth rate at linear phase. $S = 10^8$, and $S_H = \mu_0 R_0^2 v_A/\eta_H = 10^{12}$.

Nonlinear gyro-fluid simulations show results that are similar to those from the two-fluid model, namely that the P-B modes trigger magnetic reconnection, which drives the collapse of the pedestal pressure [3,4]. Hyper-resistivity is found to limit the radial spreading of ELMs by facilitating magnetic reconnection. The ELM size is found to be insensitive to the hyper-resistivity for large ELMs. Due to the additional FLR-corrected nonlinear ExB convection for the ion gyro-center density, the gyro-fluid model further limits the radial spreading of ELMs as shown in Fig.2, and the FLR effect can significantly decrease the ELM size when the pedestal ion temperature increases from 1keV to 4keV because high-n modes are stabilized. Furthermore, zonal magnetic fields are shown to arise from an ELM event and finite drift-wave convection in the generalized Ohms law.

3.3 Nonlinear simulations with equilibrium shear flow

The equilibrium $E \times B$ shear flow plays a dual role on peeling-ballooning modes and subsequently ELM crashes [5]. On one hand, the flow shear can stabilize high-n P-B modes and

twist the mode in poloidal direction, constraining the mode's radial extent and reducing the size of the corresponding ELM. On the other hand, the shear flow also introduces the Kelvin-Helmholtz mode, which can destabilize the peeling-ballooning modes. The overall effect of equilibrium shear flow on peeling ballooning modes and ELM crashes depends on the competition between these two effects. When the flow shear is either small or very large, it can reduce ELM size. However, for moderate values of flow shear, the destabilizing effect from the Kelvin-Helmholtz drive is dominant and leads to larger ELM crashes. Using a hyperbolic tangent function as a phenomenological model of the net flow with a fixed shear scale length $L_v = 3.4cm$ and constant density profile, the two-fluid simulation results are shown in Figure 3 for the ELM size and energy loss at the outboard mid-plane, as well as the corresponding linear growth rates.

4. A new non-Fourier Method for applying the Landau-Fluid operators

Tokamak edge plasmas have regions in which kinetic effects are important. This strongly motivates the implementation of Landau-fluid (LF) operators [6,7] in edge-plasma fluid codes such as BOUT++. However, they also have significant spatial inhomogeneities and complicated boundary conditions, which pose significant difficulties for the standard Fourier implementations. We have therefore developed non-Fourier, configuration-space-based approaches for the computation of these operators. A simple non-Fourier approximation to $1/|k|$ Landau-fluid operator is a truncation of a self-similar infinite sum:

$$\frac{1}{|k|} \approx \sum_{n=0}^{N} \frac{\alpha^n k_0}{k^2 + (\alpha^n k_0)^2} \qquad (18)$$

One of these is a "fast" method, with Fourier-like computational scaling, based on an approximation by a sum of Lorentzians which can be numerically implemented through the solution of tridiagonal or narrowly banded matrix equations. Certain choices of the constants α, k_0 and N give an excellent fit to $1/|k|$ in Fourier space. A spectral collocation analysis has been developed that greatly aids in the optimization of such approximations for accuracy and computational cost, across all regimes of collisionality. Fig. 4(a) shows that such an approximation using seven Lorentzians (N=7) can be accurate for the collisionless case to within 1.5% relative error over a spectral range of 5×10^3. Fig. 4(b) shows that the nonlocal flux using this method agrees well with the result from the spectral method.

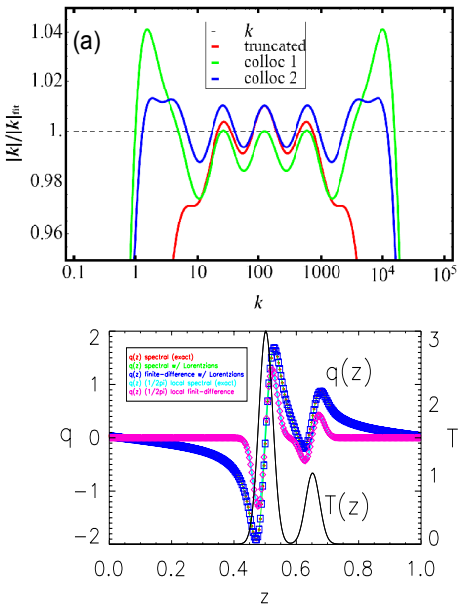

FIG. 4: . (a) ratio of actual value of $|k|$ to fit using a sum of 7 scaled Lorentzians. The "truncated" curve is for a simple truncation fit, while the "colloc" curves are for improved fits resulting from collocation analysis. (b) Comparison of the nonlocal flux resulting from a temperature profile (black dotted), computed with the exact spectral method (solid black), and sum-of-Lorentzians methods (spectral - red; finite difference - green, dashed), and the local (diffusive) flux (blue, solid).

We have also implemented and compared the computational cost of a variety of other approaches, including the Fourier approach, direct convolution, and matrix multiplication. Fig.5 shows that the fast non-Fourier approach has a computational cost scaling for large

numbers of grid cells similar to the Fourier approach. For modest numbers of grid cells, (<100), direct matrix multiplication or convolution are viable alternatives, and can be more efficient than even the Fourier approach. The fast non-Fourier approach has been implemented for the parallel LF closure in BOUT++, and implementation of the other approaches and for the toroidal LF closure is underway. These will be exercised on a variety of linear and turbulent microinstability-driven test cases.

5. Summary and Discussion

In conclusion, an isothermal electromagnetic 3-field gyro-fluid model has been developed and implemented in the BOUT++ framework to study the physics of nonlinear peeling-ballooning mode dynamics. It is found from linear simulations that retaining complete first order FLR corrections as resulting from the incomplete "gyroviscous cancellation" in Braginskii's two-fluid model [i.e., including all three terms on the second line of Eq.(15)] is necessary to obtain good agreement with gyro-fluid results for high ion temperature cases ($T_i \succeq 3keV$) when the ion density has a strong radial variation, which goes beyond the simple local model of ion diamagnetic stabilization of ideal ballooning modes. Nonlinear gyro-fluid simulations show results that are similar to those from the two-fluid model, namely that the P-B modes trigger magnetic reconnection, which drives the collapse of the pedestal pressure. Hyper-resistivity is still required in gyro-fluid simulations to facilitate magnetic reconnection. Due to the additional FLR-corrected nonlinear ExB convection for the ion gyro-center density, the gyro-fluid model further limits the radial spreading of ELMs, and the FLR effect can significantly decrease the ELM size when the pedestal ion temperature increases from 1keV to 4keV because high-n modes are stabilized. Finally, we have developed non-Fourier, configuration-space-based approaches for the computation of Landau-fluid operators. We find that the fast non-Fourier approach has a computational cost scaling for large numbers of grid cells similar to the Fourier approach.

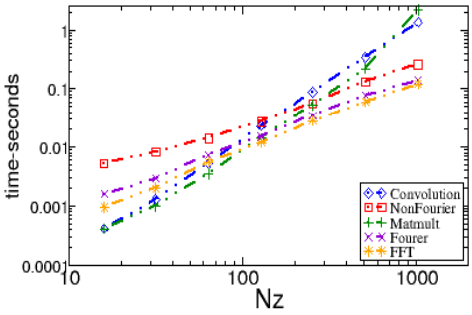

FIG. 5: Computational timings of various approaches to the application of the Landau-fluid $|k|$ operator.

Acknowledgments

The authors wish to acknowledge W. Dorland, G. W. Hammett, F. L. Waelbroeck, and H. R. Wilson for useful discussions. This work was performed for USDOE by LLNL under DE-AC52-07NA27344, LLNL LDRD project 12-ERD-022 and LDRD project 11-ERD-058, the China Scholarship Committee under contract N0.2011601099, and the China Natural Science Foundation under Contract No.10721505. LLNL-PROC-583415.

References

[1] P. B. Snyder and G. W. Hammett, Phys. Plasmas 8, 3199 (2001).
[2] X. Q. Xu, R. H. Cohen, T. D. Rognlien, et.al., Phys. Plasma 7, 1951 (2000).
[3] X.Q. Xu, et.al, Phys. Rev. Lett. 105, 175005 (2010).
[4] X.Q. Xu, et.al, Nucl. Fusion51 (2011) 103040.
[5] P. W. Xi, X. Q. Xu, et.al., Phys. Plasmas, 19, 092503 (2012).
[6] G. W. Hammett and F. W. Perkins, Phys. Rev. Lett. 64, 3019 (1990).
[7] M. A. Beer and G. W. Hammett, Phys. Plasmas 3, 4046 (1996).